

Surfactant effect on synthesis of SrAl_2O_4 nanoparticles prepared by reverse micelle process

Azita Moheb*, Saeid Abedini Khorramie and Shahram Moradi Dehaghi

Department of Chemistry, Tehran North Branch, Islamic Azad University, Tehran, Iran

Strontium aluminate (SrAl_2O_4) spinel nanoparticles were synthesized by microemulsion method using micro-reactors made of different nonionic surfactants (Span 20, Span 40 and Span 60) in a nonpolar solvent cyclohexane. The synthesized nanomaterials were characterized by X-ray diffraction (XRD) technique. The morphology of the synthesized materials was studied by field emission scanning electron microscope (FESEM). The average particles size was estimated by XRD and transmission electron microscope (TEM) with using software of IMAGE J. The effect of different surfactants on the particles size and morphology was determined. It was found that the average particles size was decreased by decreasing HLB (Hydrophilic-Lipophilic Balance) of surfactants and also the average particles size was decreased from 31 to 21 nm. HLB of surfactants is a major factor in controlling the final particles size of SrAl_2O_4 powder. Dislocation of peaks (2θ) in XRD with decreasing HLB of surfactant was decreased slightly. The XRD analysis of all the powders indicated the formation of single-phase spinel structure on calcinations.

Key words: Strontium aluminate, Nanoparticle, Span 20, 40 and 60, X-ray diffraction, Hydrophilic-lipophilic balance of surfactant.

Introduction

In 1959, Schulman originally proposed the word “microemulsion”. It is containing at least three components that is a nonpolar phase (usually oil), a polar phase (usually water) and a surfactant. Molecules of surfactant form an interfacial film separating the polar and the non-polar domains. A microemulsion is a thermodynamically stable, isotropic and macroscopically homogeneous solution [1]. Since the 1980s, the synthesis of nanoparticles by microemulsions method has been a popular research topic, when the first colloidal solutions of palladium, platinum and rhodium metal nanoparticles were prepared [2, 3].

Strontium aluminate SrAl_2O_4 is a solid odorless, nonflammable and pale yellow. It is chemically and biologically inert. Strontium aluminate cement can be used as refractory structural material. It can be used as the cement for refractory concrete for temperatures up to 2000 °C. Aluminates have attracted the attention of the research community because of their properties as high mechanical resistance, low surface acidity, thermal stability and hydrophobicity. Their properties are suitable for many applications, such as ceramics, optical, magnetic, catalysts and carriers for active metal [4-6]. Ceramic alkaline earth aluminates have captured considerable attention because of their excellent photoluminescence, radiation intensity, color purity and

good radiation resistance [8]. The spinel structure SrAl_2O_4 is famous because of long-persisting phosphors. These phosphors had been applied such as luminous watches, exit signs, decorative items, traffic signs, military applications, emergency passageway illumination, lighting equipment and low level lighting [8, 9]. Strontium aluminate can apply or act as a host for lanthanide ions when it co-doped with Dy^{3+} exhibits remarkable optical characteristics [10, 11]. And also, it co-doped with europium and dysprosium ($\text{SrAl}_2\text{O}_4: \text{Eu}^{2+}, \text{Dy}^{3+}$) are applied in many fields because of their excellent phosphorescence [12]. It is used in signposts, billboards, road signs, emergency lighting, interior design and safety indication [13-15]. This material can be applied to preparation new metal compound composites [16]. They exhibit photocatalytic activity because of their photosensitive properties [17, 18].

SrAl_2O_4 and BaAl_2O_4 nanoparticles have successfully prepared by many different methods, such as via the sol-gel methods [19-22], hydrothermal reaction methods [18, 9], high temperature solid state reaction [23-25], co-precipitation methods [26, 27], $\text{SrAl}_2\text{O}_4: \text{Eu}^{2+}, \text{Dy}^{3+}$ synthesized by hydrothermal reaction [18] and combustion method [9].

It was reported that the particles size is affected by surfactant and co-surfactant type has been investigated [28-30]. Also, the effect of different solvents has been investigated [28, 31-33]. Several studies have shown that reactant concentration in particles size is effective [35-37]. Many articles show the final particles size is dependent on the initial water to surfactant molar ratio $W_0 = [\text{H}_2\text{O}] / [\text{Surfactant}]$ [37-45]. The studies are

*Corresponding author:
Tel : +98-912-1225116
Fax: +98-2177009848
E-mail: a.moheb@iau-tub.ac.ir

reported that the size of final particles is changed insignificantly by the addition of electrolyte [46, 47].

In this paper, strontium aluminate nanoparticles were synthesized by microemulsion method and influence of different surfactants on the particles size of SrAl_2O_4 powder was reported. XRD was used in order to check the crystalline phases of the particles, morphologies and size of particles are characterized using FESEM and TEM.

Experimental

Strontium nitrate anhydrous ($\text{Sr}(\text{NO}_3)_2$, 99%, Merck), aluminum nitrate nonahydrate ($\text{Al}(\text{NO}_3)_3 \cdot 9\text{H}_2\text{O}$, 98.5%, Merck) were used as the precursor of strontium and alumina, respectively. The required amount of strontium nitrate and aluminum nitrate salts (Sr: Al =1:2) was dissolved in deionized water to a concentration of 0.1 M. Cyclohexane (99.5%, Merck) was used as an organic solvent.

A solution of reverse microemulsion was prepared by mixing 0.09 M of sorbitan monolaurate (Span 20, Merck) a nonionic surfactant, 0.93 M of cyclohexane and 0.1 M of mixed aqueous salt solution.

B solution of reverse microemulsion was prepared by mixing 0.09 M of sorbitan monopalmitate (Span 40, Sigma Aldrich) a nonionic surfactant, 0.93 M of cyclohexane and 0.1 M of mixed aqueous salt solution.

C solution of reverse microemulsion was prepared by mixing 0.09 M of sorbitan monostearate (Span 60, Sigma Aldrich) a nonionic surfactant, 0.93 M of cyclohexane and 0.1 M of mixed aqueous salt solution. The microemulsion was mixed rapidly, and after 30 min of equilibration 0.2 M of NH_4OH (28%, Merck) was injected into the microemulsion. Then, the microemulsion was centrifuged to extract the particles and they were subsequently washed by ethanol to remove any residual surfactant. The powders were dried at 60 °C in an oven for 24 h, then ground and calcined at 1000 °C for 2 h. Fig. 1 shows the flowchart for the preparation of SrAl_2O_4 nanopowders by reverse micelle processing. The phase identification of calcined powders was recorded using X-ray diffractometer (STOE STADI, MP) that is shown in Fig. 2. The morphology of the calcined powder was observed by FESEM operating at an accelerating voltage of 30 KV (MIRA3 TESCAN) that is shown in Fig. 3.

The particles size of the calcined powders was analyzed using TEM operating at an accelerating voltage of 200 KV (Philips, CM30) by placing the powder on a copper grid to get the details about the morphology and size of the powders that is shown in Fig. 4.

The average size of the particles was estimated from the TEM micrographs using standard software IMAGE J that is shown in Fig. 5.

The crystallite size of the calcined SrAl_2O_4 powder

was calculated from full width at half maximum (FWHM) peak using Scherrer's equation [48].

Results and Discussions

The XRD patterns of the calcined samples are reported with different surfactants at 1000 °C for 2 hrs in Fig. 1. The detected diffraction peaks are corresponded to the standard patterns of SrAl_2O_4 (ICSD card 00-031-1336). All the samples were found to have a hexagonal crystal structure. According to this analysis, all three patterns show the formation of single phase SrAl_2O_4 . No other crystalline phase was found in the calcined samples. Location of peaks (2θ) in XRD with decreasing HLB of surfactants was decreased. The average nanoparticles size was calculated by the following Scherrer's equation.

$$D = \frac{k\lambda}{\beta \cos \theta} \quad (1)$$

In the equation, D is the size of the crystallite sample, λ is the wavelength of X-ray source of Cu- K_α (1.54 Å), k is the Scherrer's constant (0.9), β of FWHM is the

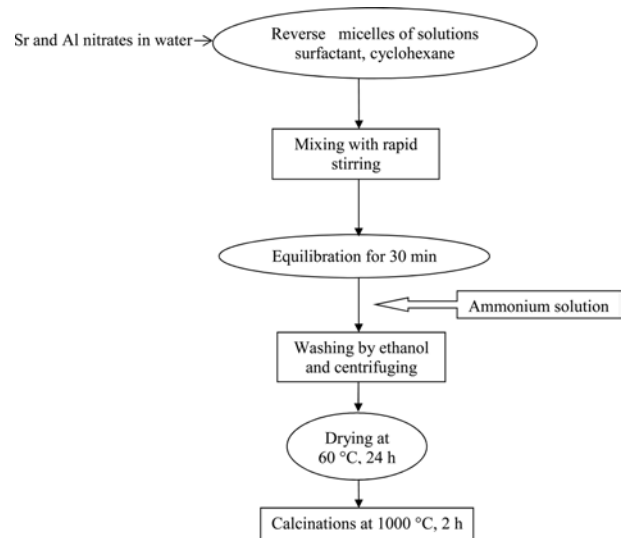


Fig. 1. Flowchart for the preparation of nanoparticles by reverse micelle processing.

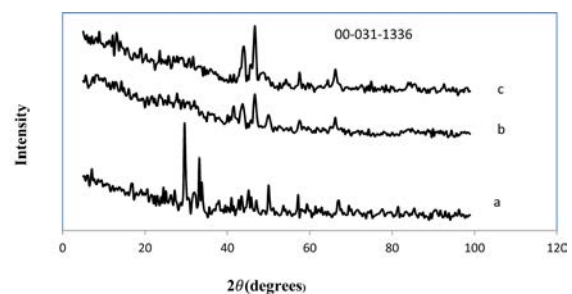


Fig. 2. X-ray diffraction patterns of SrAl_2O_4 powder calcined with different solvents, a: Span 20, b: Span 40 and c: Span 60.

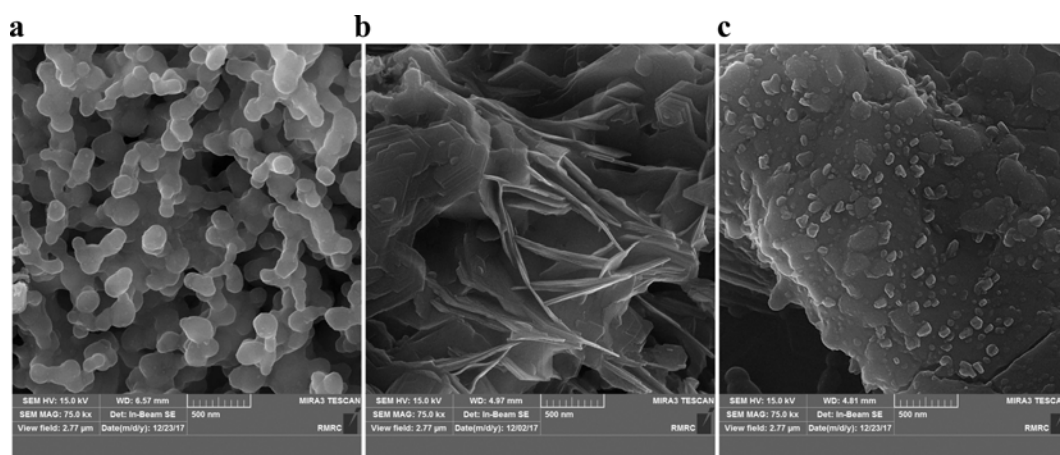


Fig. 3. FESEM images of SrAl₂O₄ powder calcined at 1000 °C for 2 hrs, a: Span 20, b: Span 40 and c: Span 60.

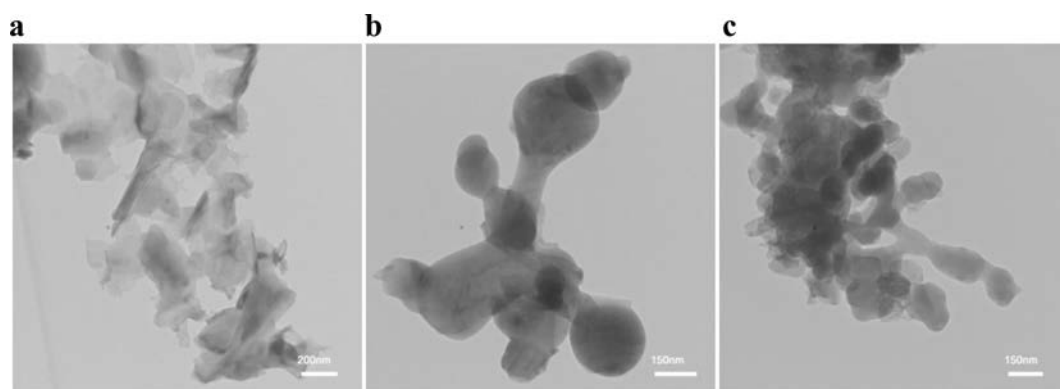


Fig. 4. TEM micrographs of SrAl₂O₄ powder calcined at 1000 °C for 2 hrs, a: Span 20 b: Span 40 and c: Span 60.

width at half its maximum intensity and θ is the half diffraction angle at which the peak is located. The result shows that the size of the synthesized nanoparticles with decreasing HLB of surfactant from HLB = 8.6 (Span 20), HLB = 6.7 (Span 40) and to HLB = 4.7 (Span 60) were decreased from 31 to 21 nm, respectively. Table 1 shows the data of Scherer's equation and the dislocation value.

The surface morphology of samples was reported by FESEM. The FESEM micrographs of SrAl₂O₄ nanopowders in different surfactants show that the particles are not uniform in shape. FESEM images show that at Span 20 surfactant the boundary between phases is clear and also density of the particles is more than the other images. At Span 40, shape of particles are as sheet and are not clung to each other and also at Span 60 surfactant, they are sheet but are clung to each other. Meanwhile, the boundary between phases with decreasing HLB of surfactants was decreased. In the FESEM images due to the presence of moisture in the environment, agglomeration between nanoparticles are observed.

Fig. 4 shows the TEM micrographs and size distribution of nanoparticles. These samples were synthesized with different surfactants and cyclohexane

Table 1. Scherer's data information for SrAl₂O₄ nanoparticles.

Samples	β_{obs} (2θ)	Peak position (2θ)	Crystallite size (nm)	Type of crystallite
Span 20	0.266	29.617	31	hexagonal
Span 40	0.370	29.356	22	hexagonal
Span 60	0.384	28.200	21	hexagonal

as an organic solvent and then they were calcined at 1000 °C for 2 hrs. All the particles are very fine. TEM images show that the most of SrAl₂O₄ nanoparticles synthesized at Span 20 are nearly spherical, at Span 40 are completely spherical and at Span 60 are spherical. The average size of the particles estimated from the TEM image using standard software IMAGE J is found to decrease with decreasing HLB of surfactant. The average size of nanoparticles from HLB = 6.7 (Span 20) HLB = 6.7 (Span 40) to HLB = 4.7 (Span 60) are decreased, respectively. The nanoparticles size distribution in different surfactant is similar to each other Fig. 5.

Decreasing of the average size of nanoparticles is agreement with crystallite size data of the targets calculated by Scherer's equation. Results of experiment

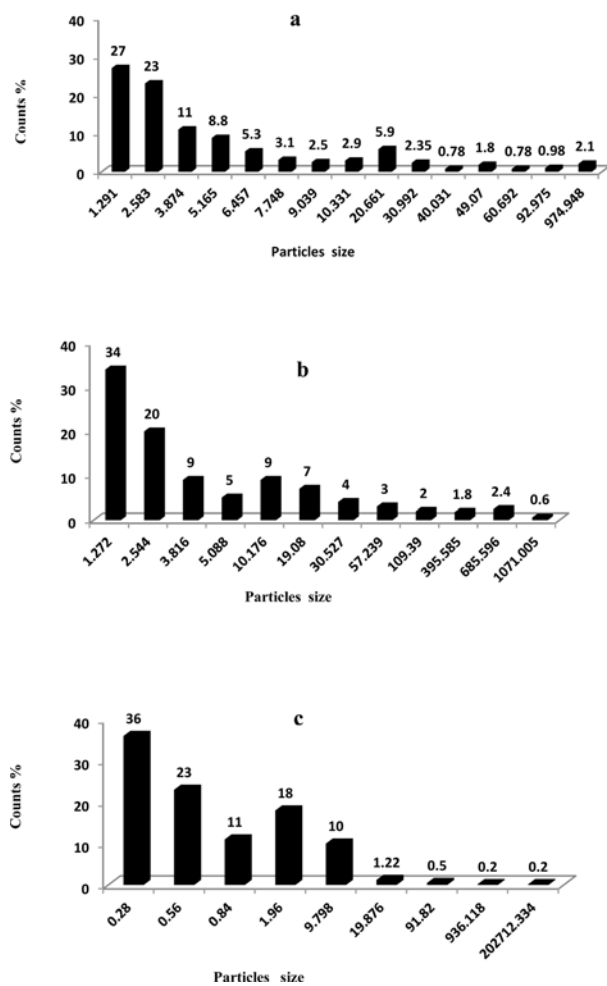


Fig. 5. Diagram of particles distribution of SrAl_2O_4 was estimated by using software IMAGE J, a: Span 20 b: Span 40 and c: Span 60.

show that the HLB of surfactant can control the diameter of the nanoparticles in the microemulsion.

Conclusions

SrAl_2O_4 nanoparticles can be synthesized by reverse micelle processing at 1000°C for 2 hrs. All the calcined powders show the presence of hexagonal phase and no other crystalline phase are found in the samples. The surfactant of Span 20, Span 40 and Span 60 is effective on the particles size distribution of nanoparticles. The particles size can be controlled by changing HLB of different nonionic surfactants. Dislocation of peaks (2θ) in XRD with decreasing HLB of surfactant was decreased slightly. The results of the TEM are agreement with the XRD results. The presence of moisture in the environment causes agglomeration of nanoparticles. The average particles size of SrAl_2O_4 was found to decrease with decreasing of surfactant hydrophilic-lipophilic balance.

References

1. M. Amaik, M. Younuswani, and M.A. Hashim, Arab. J. Chem. 5 (2012) 397- 417.
2. M. Boutonnet, J. Kitzling, P. Stenius, and G. Maire, J. Colloids. Surf. 5 (1982) 209-225.
3. J. Eastoe, M.J. Hollamby, and L. Hudson, Adv. Colloid Interface Sci. 128-130 (2006) 5-15.
4. X. Duran, M. Pan, F. Yu, and D. Yuan, J. Alloys. Compd. 509 (2011) 1079-1083.
5. D. Dhak, and P. Pramanik, J. Am. Ceram. Soc. 89 (2006) 1014-1021.
6. C. Ragupathi, J. Judith Vijaya, L. John Kennedy, and M. Bououdina, J. Ceram. Int. 40 (2014) 13067-13074.
7. H. Du, W. Shan, L. Wang, D. Xu, H. Yin, Y. Chen, and D. Guo, J. Lumin. 176 (2016) 272-277.
8. C. Zollfrank, S. Grabow, H.D. Kurland, and F.A. Müller, J. Acta. Mat. 61 (2013) 7133-7141.
9. A.K. Bedyal, V. Kumar, O.M. Ntwaeaborwa, and H.C. Swart, J. Rad. Phys. Chem. 122 (2016) 48-54.
10. C. Zollfrank, S. Grabow, H.D. Kurland, and F.A. Müller, J. Acta. Mat. 61 (2013) 7133- 7141.
11. H. Yamada, K. Nishikubo, and C. Xu, J. Electrochem Soc. 155:F (2008) 139-144.
12. C.A. D'Amato, R. Giovannetti, M. Zannotti, E. Rommozzi, S. Ferraro, C. Seghetti, M. Minicucci, R. Gunnella, and A. Di Cicco, J. Appl. Surf. Sci. 441 (2018) 575-587.
13. T. Katsumata, T. Nabae, K. Sasajima, and T. Matsuzawa, J. Cryst. Growth. 183 (1998) 361-365.
14. T. Nakamura, K. Kaiya, N. Takahashi, T. Matsuzawa, C.C. Rowlands, V. Beltran- Lopez, G.M. Smith, and P.C. Riedi, J. Mater. Chem. 10 (2000) 2566-2569.
15. Y. Lin, Z. Tang, and Z. Zhang, Mater. Lett. 51 (2011) 14-18.
16. T.S. Singh, and S. Mitra. J. Lumin. 127 (2007) 508-514.
17. B. Kiss, T.D. Manning, D. Hesp, C. Didor, A. Taylor, D.M. Pickup, A.V. Chadwick, H.E. Allison, V.R. Dhanak, and J.B. Claridge, J. Appl. Catal. B Environ. 200 (2017) 547-555.
18. B.G. Park, J. Catal. 8 (2018) 227-237.
19. M. Ayari, V. Paul-Boncour, J. Lamloumi, H. Mathlouthi, and A. Percheron-Guégan, J. Alloy. Compd. 420 (2006) 251-255.
20. C. Peng, T. Huajan, L. Yang, and H. Yan, J. Mater. Chem. Phys. 85 (2004) 68-72.
21. E. Cordoncillo, B. Julian-Lopez, M. Martinez, M.L. Sanjuán, and P. Escribano, J. Alloy. Compd. 484 (2009) 693-697.
22. R.J. Wiglus, and T. Grzyb, Opt. Mater. (Amst). 36 (2013) 539-545.
23. N. Suriyamurthy, and B.S. Panigrahi, J. Lumin. 128 (2008) 1809-1814.
24. Z. He, X. Wang, and W.M. Yen, J. Lumin. 119-120 (2006) 309-313.
25. H.S. Roh, I.S. Cho, J.S. An, C.M. Cho, T.H. Noh, D.K. Yim, D.W. Kim, and K.S. Hong, Ceram. Int. 38 (2012) 443- 447.
26. M.V. Rezende, P.J. Montes, F.M. Soares, C. Santos, and M.E. Valerio, J. Synchrontron. Radiat. 21 (2014) 143-148.
27. M. Momayezan, M. Ghashang, and S.A. Hassanzadeh-Tabrizi, Bulg. Chem. Commun. 47 (2015) 809-815.
28. M. Lopez-Quintela, C. Tojo, M. Blanco, L. Garcia Rio, and I. Leis, Curr. OPin. Colloid Interface Sci. 9 (2004) 264-278.
29. V. Uskokovic, and M. Drogenik, Surf. Rev. Lett. 12 (2005)

- 239-277.
30. A. Bumajdad, M. Zaki, J. Eastoe, and L. Pasupulety, *Langmuir*. 20 (2004) 11223-11233
 31. C. Kitchens, M. McLeod, and C. Roberts, *J. Phys. Chem. B*. 107 (2003) 11331-11338.
 32. J. Cason, M. Miller, J. Thompson, and C. Roberts, *J. Phys. Chem. B*. 105 (2001) 2297-2302.
 33. R. Bagwe, and K. Khilar, *Langmuir*. 13 (1997) 6432-6438.
 34. I. Lisiecki, and M.P. Pileni, *Langmuir*. 19 (2003) 9486-9489.
 35. J. Eastoe, S. Stebbing, J. Dalton, and R. Heenan, *Colloids Surf. A Physicochem. Eng. Asp.* 119 (1996) 123-131.
 36. M. Maillard, S. Giorgio, and M.P. Pileni, *J. Phys. Chem. B*. 107 (2003) 2466-2470.
 37. Y. Berkovich, A. Aserin, E. Wachtel, and N. Garti, *J. Colloid Interface. Sci.* 245 (2002) 58-67.
 38. D. Zhang, X.M. Ni, H.G. Zheng, Y. Li, X. Zhang, and Z.P. Yang, *Mater. Lett.* 59 (2005) 2011-2014.
 39. K. Kimijima, and T. Sugimoto, *J. Colloid Interface Sci.* 286 (2005) 520-525.
 40. A. Nanni, and L. Dei, *Langmuir* 19 (2003) 933-938.
 41. D. Markovec, A. Kosak, A. Znidarsic, M. Drofenik, and M.J. Magn, *J. Magn. Mater.* 289 (2005) 32-35.
 42. J. Lemyre, and A. Ritcey, *Chem. Mater.* 17 (2005) 3040-3043.
 43. L. Levy, D. Ingert, N. Feltin, V. Briois, and M.P. Pileni, *Langmuir*. 18 (2002) 1490- 1493.
 44. J. Chandradass, M. Balasubramanian, and D. SikBae, J. Kim, K. Kim, *J. Alloys. Compd.* 491 (2010) L25-L28.
 45. J. Chandradass, and K. Kim, *J. Cryst. Growth.* 311(2009) 3631-3635.
 46. C. Kitchens, M. McLeod, and C. Roberts, *Langmuir*. 21 (2005) 5166-5173.
 47. C. Saiwan, S. Krathong, T. Anukulprasert, and E. O'RearIII, *J. Chem. Eng. Jpn.* 37 (2004) 279-285.
 48. B.D. Cullity, *Elements of X-ray Diffraction*, 2nd ed, Addison-Wesley, London, UK, (1978).